Differences between the CO and NO Properties for Stability of Alkali Metal Complexes $Me(XO)_n^+$, X = C or N

ALEXANDER V. LARIN,[1,2] DMITRII N. TRUBNIKOV,[2] DANIEL P. VERCAUTEREN[1]

[1]*Institute for Studies in Interface Sciences, Laboratoire de Physico-Chimie Informatique, Facultés Universitaires Notre Dame de la Paix, Rue de Bruxelles 61, B-5000 Namur, Belgium*
[2]*Laboratory of Molecular Beams, Department of Chemistry, Moscow State University, Vorob'evu Gory, Moscow, B-234, 119899, Russia*

ABSTRACT: The influence of electron density redistribution upon vibrational excitation $v \leftarrow 0$ on the interaction energy between CO and the metal atom Me in $Me(CO)_n^+$ carbonyls, $n = 1$–3, is discussed. It is shown that the decrease of the CO dipole in the carbonyls upon vibrational excitation is qualitatively similar to the one of CO in the gas state. The respective decrease of the total energy of carbonyl complexes mainly due to the electrostatic repulsion Me^+–C^+O^- ($v > 6$) is estimated herein for positively charged carbonyl complexes with Me = Li, Na, K, or Rb, upon the proposition of a strong coupling between the CO vibration and the electronic excitation of the whole complex. The difference between the NO and CO ligands with respect to their vibrational excitation is discussed. Also the appearance of angular bicarbonyls in adsorbed state in zeolite frameworks is considered.   © 2002 John Wiley & Sons, Inc. Int J Quantum Chem 00: 1–8, 2002

Key words: !! PLEASE SUPPLY !!!

Introduction

The appearance of bicarbonyl (CO)Na(CO) species with opposite CO– or OC– attachment was recently proposed through the interpretations of the vibrational frequencies of CO adsorbed in different cationic forms of the FER and ETS-10 zeolite frameworks [1, 2]. Similarly, for $^{15}N_2$/CO mixtures adsorbed in NaY, the band at 2167 cm^{-1} was assigned to an analogous $(^{15}N_2)$Na(CO) carbonyl complex [3].

Alkali metal carbonyl (AMCs) cations are important models for the understanding of such complicated processes. They indeed can provide instructive explanations for the adsorption of simple gases, for which the main energetic aspects of adsorption can be explained at the level of isolated Me^{+1}–XY pairs, where Me is a transition or an alkali metal atom, and XY = CO or NO [4–6]. Despite the fact that bicarbonyls as well as mixed AMCs are of relatively small size and thus could be easily considered with high-level computations [4–6], no systematic study of the opposite CO and OC attachment has, to our knowledge, been performed so far. Still, theoretical analyses of the variation of the lower frequency modes can indeed help in the assignment of the observed satellites in their spectra.

Another advantage of the AMCs is that they present analogous models to the transition metal carbonyls (TMCs) but wherein the Me–CO bonding is not supplied by π backdonation [7]. As we have recently shown, the decrease of the interaction energy (IE) between Me(CO)$_{n-1}$L and CO ($v > 6$), with Me = V, Ti, or Cr, and L = CN or Cl, in the excited vibrational v states of CO is comparable to the experimental CO dissociation energy from the excited electronic states of Me(CO)$_n$L^{+q} while $q = 0$ and 1, and $n > 1$ [8]. This correlation allowed us to suggest the "electrostatic" nature for the CO dissociation from Me(CO)$_n$L^{+q} complexes in excited electronic states. Such interpretation is related to the charge distribution analysis [9, 10] of the atoms of the carbonyl complex. Provided that the coupling between the electronic excitation of the TMCs and the vibrational excitation of CO (in axial position in multicarbonyls) is strong enough, the occupation of the high vibrational states of CO should lead to a strong variation of the electron density distribution as compared to the ground state and to the elimination of CO owing to repulsive (CO)$_{n-1}$LMe–CO interactions [8]. In relation, the case of the AMCs allows an easy illustration for such types of carbonyl

reactions owing to a larger charge on the metal atom as compared to within the TMCs.

In this work, we particularly tackle the CO elimination phenomenon in AMCs. The geometries of the AMC complexes were studied with respect to the number of CO molecules and cation type. In the next part, we explain the model adopted to evaluate the stability of the carbonyls in their excited states with respect to CO dissociation. In the results part, we discuss their stability and then compared the behavior of CO in the monocarbonyl K(CO)$^+$ cation to the one of NO in K(NO)$^+$, wherein NO changes its dipole sign at larger internuclear distances (ρ). The last part of the results is devoted to the stability of sodium bicarbonyls found to adsorb in several zeolites.

Computational Details

The geometries of the Me(XO)$_n^+$ complexes, with Me = Li, Na, K, or Rb and X = C or N, were fully optimized at the density functional theory (DFT) and the second-order Møller–Plesset (MP2) levels of theory using the GAUSSIAN98 [11] and GAMESS [12] codes, respectively. The cc-pVTZ basis set was used on all C, N, O, and Cl atoms, and the 6-311G** basis on the Me atoms. The consideration of electron correlation as well as a high-quality basis set was necessary to provide an accurate description of the behavior of the CO dipole moment with its internuclear distance ρ (Table I). Doing so, a small advantage of most DFT functionals as compared to MP2 was noted while applying the cc-pVTZ basis set. The slope of the CO dipole versus its internuclear distance is indeed relatively underestimated with MP2 while it is only slightly overestimated with the B3P86 functional as compared to the experimental slope [8]. Hence, DFT and MP2 methods lead to values that could be considered as upper and lower bounds for the CO dipole moment, respectively. The optimized carbonyl geometries were then used for single-point computations at fixed Me–CO distance in the various vibrational excited states. For NO, one can observe a close coincidence between the experimental and calculated dipoles, frequencies, and geometries.

We hypothesize that, owing to a strong electronic-vibrational (vibronic) coupling, the geometry of all Me(XO)$_n^+$ complexes in their excited electronic states relaxes quickly to one of the ground states with the exception of one XO ligand. That is why the stability of the "relaxed" complexes should be

TABLE I

Properties of the XO molecule, X = C or N, optimized with different basis sets: X–O equilibrium distance ρ_e (Å), dipole moment μ (1 a.u. = 1 ea_0), Mulliken atomic charge $q(X) = -q(O)$ (1 a.u. = 1 e), and harmonic vibrational frequency ω_e (cm^{-1}).

Basis set	Method	ρ_e	μ	$-q(X)$	ω_e[a]
CO					
cc-pVTZ	BHandHLYP	1.1134	0.0098	0.003	2258
	B3PW91	1.1260	0.0582	0.019	2156
	B3P86	1.1253	0.0540	0.019	2160
	MP2	1.1380	0.1154	0.076	2125
[6s4p4d2f][b]	BHandHLYP	1.1183	−0.0113	0.163	2259
	B3PW91	1.1312	0.0379	0.254	2154
	B3P86	1.1306	0.0346	0.257	2159
	MP2	1.1387	0.1108	1.193	2124
Experiment		1.13[c]	0.0481[d]	—	2170[c]
NO					
cc-pVTZ	B3PW91	1.1435	0.0495	0.0014	1945
	B3P86	1.1429	0.0488	0.0005	1948
Experiment		1.149[c]	0.0622[e]	—	1904[c]

[a] Harmonic DFT frequencies are scaled by 0.9716 as in Ref. [13]; no scaling for MP2.
[b] Basis set from Ref. [14].
[c] Ref. [15].
[d] Ref. [16].
[e] Ref. [17].

determined with respect to the energy of the ground state. As a measure of the stability, the energy variation of the interaction energy between Me(XO)$_{n-1}^+$ and XO in the vibrational excited states of the XO molecule was calculated as:

$$\Delta U = U(\rho_v) - U(\rho_0), \tag{1}$$

where $U(\rho_0)$ is the total energy of the Me(XO)$_n^{+q}$ carbonyl complex with all XO molecules in the ground state and $U(\rho_v)$ is the total energy of Me(XO)$_{n-1}$(XO*)$^{+q}$ with one XO molecule in the excited vibrational v state, ρ_v corresponding to the average XO internuclear distance at the v state. In this work, we admitted that $\rho_0 = \rho_e$, ρ_e being the equilibrium XO distance, because the small correction $U(\rho_0) - U(\rho_e)$ would require a huge effort of evaluation for the anharmonicities of each complex.

To evaluate the energy variation (1) in the case of the XO complexes, one should thus be precise about the excited vibrational v state. This correct estimation requires the calculation of ρ_v for each particular carbonyl complex considering the perturbed potential curve of isolated CO vibration in the complex. For simplicity, a unique conventional value of $\rho_v = 1.27$ Å (2.40 a.u.) was accepted as the average distance for the XO excited state for all complexes.

This ρ_v value corresponds nearly to the $v = 17$ state for the independent one-dimensional CO vibration and only to the $v = 13$ state for NO in the gas state on the basis of anharmonicity parameters taken from Ref. [18]. With the energy estimations using the LEVELS code [19] (Table II), one can evaluate that the respective excitation energies are located in the ultraviolet (UV) and visible regions for CO (32883.2 cm^{-1}) and NO (21811.6 cm^{-1}), respectively. The distance $\rho_v = 1.27$ Å could correspond to a lower v state than 17 and 13, respectively, if a "blue" band shift is observed for the XO vibration as it is usually observed in the AMCs (Table III). The final vibrational state of the XO molecule owing to the coupling in any excited electronic state of the complex will depend on the energy of the electronic excite state with respect to the energies of the vibrational states of the XO molecule. The $\rho_v = 1.27$ Å approximation allows to evaluate qualitatively the stability of the complex including the highly excited XO molecule. A comparison between the ΔU values calculated upon such ρ_v and ρ_0 choice and the experimental dissociation data [7, 21] for the CO molecules from the AMCs is made in the following part.

Energies of vibrational states ν (in cm^{-1} relative to the potential minimum) of CO and NO molecules in the gas state.[a]

State ν	CO	NO
0	1081.82	946.59
1	3225.15	2822.67
2	5341.98	4668.57
3	7432.38	6483.59
4	9496.42	8266.88
5	11534.17	10017.68
6	13545.72	11735.19
7	15531.13	13418.63
8	17490.48	15067.21
⋮	⋮	⋮
13	26899.11	22758.21
14	28703.76	24180.03
15	30482.92	25560.94
16	32236.66	26900.01
17	33965.06	28196.22
18	35668.22	29448.62
19	37346.22	30656.05
20	38999.14	31817.48
21	40627.08	32931.97
22	42230.11	33997.45
23	43808.32	35013.54
24	45361.78	35978.58

[a] From Mattera potential [20] for CO curve and improved Morse potential [18] for NO curve with LEVELS code [19].

Results

First, we emphasize some computational aspects of the results presented in Table III. A slight influence of the LANL2 [11] or SBK [12] effective core potentials used for the Me atom (also for C and O with SBK) on the calculated values was observed for the $K(CO)_2^+$ and $Li(CO)_2^+$ carbonyls, respectively. The lower energy variation values [Eq. (1)] evaluated with MP2 are in agreement with our previous calculations for the TMCs [8] as well as with the behavior of the CO dipole at the MP2 level of computation.

The main results are that the energy variation ΔU values [Eq. (1)] are relatively large as compared to the experimental $Me(CO)_{n-1}^+$–CO dissociation energies [7], i.e., between 7.9 kcal/mol for K^+–CO and 13.6 for Li^+–CO, and between 6.0 kcal/mol for the $Na(CO)^+$–CO case and 8.4 for $Li(CO)_2^+$–CO. So, if any energy of the carbonyl complex in an excited

electronic state could be transferred to the vibrational degree of freedom of the CO molecule, then CO could dissociate.

To understand if the proposed mechanism of dissociation from the excited electronic states of the carbonyl complexes could also be valid for other ligands than CO, we next calculated the respective variations for NO under the same conditions. For the cation complexes studied herein, the variation of the Me and CO charges upon vibrational excitation is very minor as already shown for the TMC cations [8], so that the electrostatic repulsion is mainly determined by the charge–dipole term. The charge–quadrupole is of minor importance owing to opposite variations of the Me charge (decrease) and CO quadrupole moment (increase) upon excitation. Hence, we evaluated the XO dipole moment μ in all $Me(XO)_n^+$ complexes from the X and O atomic Mulliken charges, where X = C or N. In Figure 1, one can compare the NO dipole dependence versus the internuclear distance ρ calculated from the Mulliken charges with the precise DFT dependence, which is in agreement with the experimental value at ρ_e. Even if the dipole calculated on the basis of the Mulliken atomic charges deviates from the correct dependence, it reproduces its qualitative behavior,
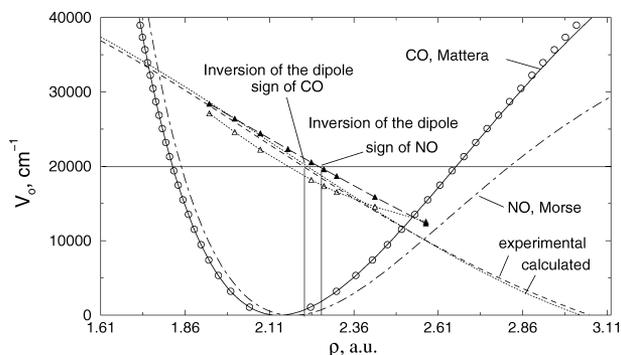
FIGURE 1. Potential energy V_0 and dipole moment μ (scaled as $\mu \times 60,000 + 20,000$ to have a common scale with V_0) with respect to the internuclear X–O distance ρ in the gas state. CO: Mattera curve [20] (solid line) and Rydberg–Klein–Rees points (open circles) [19] together with the dipole dependences calculated at the SDQ-MP4/[6s4p4d2f] level (short dashed line) [14] compared to the experimental dipole dependences $\mu(\rho)$ (long dashed line) [22] relative to the zero dipole value (corresponding to the solid line at 20,000 cm^{-1}). NO: improved Morse curve (dotted-dashed line) [18] and dipole moment calculated at the B3PW91/cc-pVTZ level (filled triangles) and from respective Mulliken charges (open triangles).

TABLE III

Properties of the $Me(XO)_n^+$ cation complexes, where X = C or N, optimized with the 6-311G**(Me)/cc-pVTZ(N,C,O) basis set.[a]

Complex	Method	R	ρ_e	q(Me)	ω_e[b]	ΔU
Li(CO)	B3PW91	2.183	1.115	0.878	2253.7	26.8
Li(CO)$_2$	B3PW91	2.203	1.116	0.802	2247.3, 2247.4	26.5
Li(CO)$_2$	B3P86	2.197	1.115	0.807	2251.1, 2251.2	26.8
Li(CO)$_2$[c]	MP2	2.195	1.131	0.646	2178.2, 2180.0	19.6
Li(CO)$_3$	B3LYP	2.210	1.117	0.705	2232.6, 2233.5	25.8
Na(CO)	B3PW91	2.605	1.117	0.926	2230.6	25.5
Na(CO)$_2$	B3PW91	2.621	1.118	0.851	2219.5, 2220.0	25.4
Na(CO)$_2$	B3P86	2.603	1.117	0.850	2232.2, 2232.7	25.7
Na(CO)$_2$	B3LYP	2.593	1.118	0.822	2219.5, 2220.0	25.1[c], 24.9
Na(CO)$_2$[c]	MP2	2.617	1.132	0.772	2163.9, 2164.7	18.9[d], 19.2
Na(CO)(OC)	B3PW91	2.640	1.117	0.866	2092.0, 2227.4	—
Na(CO)(N$_2$)	B3PW91	2.612	1.118	0.864	2227.4, 2403.6	—
Na(NO)$_2$	B3PW91	2.540	1.137	0.907	1787.0, 1974.4	—
K(CO)	B3PW91	3.101	1.119	0.971	2212.2	24.5
K(NO)	B3PW91	2.925	1.136	0.966	1995.4	17.6
K(CO)$_2$	B3PW91	3.115	1.120	0.940	2208.5, 2209.4	24.4
K(CO)$_2$[e]	B3PW91	3.123	1.120	0.944	2216.7, 2217.1	24.4
K(CO)$_2$[c]	MP2	3.142	1.134	0.935	2151.7, 2152.0	18.3
Rb(CO)[e]	B3PW91	3.417	1.120	0.982	2203.5	24.1
Rb(CO)$_2$[e]	B3PW91	3.429	1.121	0.964	2202.1, 2202.4	24.0

[a] $R = |Me–X|$ distance, X–O equilibrium distance ρ_e(Å), Mulliken atomic charge q(Me) (a.u.), harmonic vibrational frequency ω_e (cm^{-1}), and energy variation ΔU (kcal/mol) upon one XO excitation.

[b] Harmonic DFT frequencies are scaled by 0.9716 [13], no scaling for MP2, lower and higher frequencies correspond to symmetric and asymmetric vibrations, respectively.

[c] Pseudopotential SBK(Me,C,O) basis set [12].

[d] The estimation corresponds to half of the ΔU value upon the excitation of both CO molecules at the C_{2v} configuration when the distance between the CO molecules is large enough to allow us to justify the estimation of the dipole–dipole interaction via multipole series and to disregard its increase (less than 10^{-3} kcal/mol).

[e] Pseudopotential LANL2 (Me) basis set [11].

and we can consider the "Mulliken" dipole as a conventional value for comparison between the KCO$^+$ and KNO$^+$ complexes (Fig. 2).

The dependences of the Mulliken dipole moment μ versus the internuclear XO distance in the K$^+$–XO complexes (circles in Fig. 2) are compared to the known gas state dependence (diamonds) of CO [14, 22] and NO calculated herein. The dipole moment of CO in the carbonyls reveals a similar behavior with the gas state dipole, but has a more pronounced slope variation and changes its sign at a larger internuclear CO distance (ρ around 1.20 Å, 2.27 a.u.) as compared to the gas state (around 1.175 Å, 2.22 a.u.) and at a shorter ρ value as compared to the NO ligand (around 1.23 Å, 2.32 a.u.). These different internuclear distances for the change of sign of the CO and NO dipoles suggest different degrees of vibrational excitation of the XO molecule

in the excited electronic states of their respective complexes $Me(XO)_n^+$. Both the larger experimental vibrational frequency of CO, i.e., 2170 instead of 1904 cm^{-1}, as well as the smaller ρ value where the dipole inversion takes place, mean that this excitation should occur at essentially lower vibrational states than for NO.

If one displays the energy variation ΔU with respect to the XO dipole in the vibrational excited states (Fig. 3), a sharper energy decrease is emphasized for NO, from the left of $\rho = 0$ to the negative values. But the same value for the NO dipole moment in the vibrational excited states can be achieved at much higher vibrational states than for CO. Owing to the closeness of these upper vibrational states, the life time of the respective vibrational states will probably be very small and the possibility to populate these vibrational states from
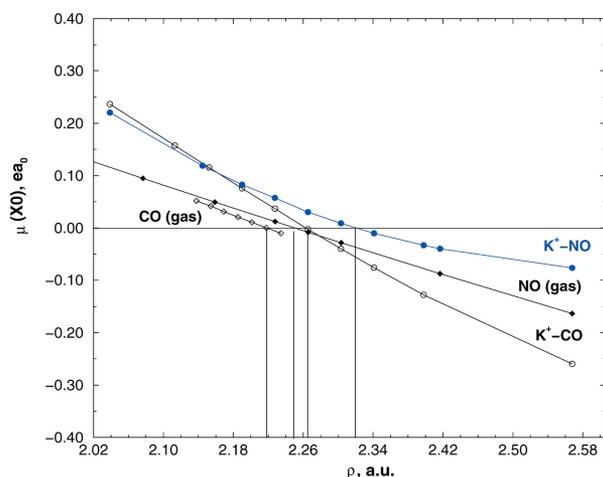
FIGURE 2. XO dipole moment versus the internuclear XO distance ρ in the K–XO$^+$ complex, where X = C (open circles) or N (filled circles). Gas state dipole: CO in vibrational states $\nu = 0$–6 (open diamonds, calculation of energies and ρ_ν with the LEVELS code [19]); NO (filled diamonds, calculated at the B3PW91/cc-pVTZ level).

the electronic excited ones of same energy could also be lower.

We already showed that the CO elimination from the electronically excited TMCs due to a coupling between the vibrationally excited CO and the electronically excited states of the complex is possible [8]. This additional study confirms that the coupling can also be effective for the electronically excited states of the AMCs, even if there is, to our
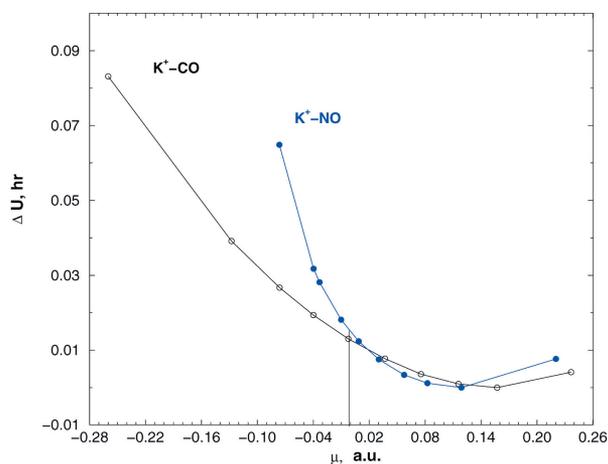
FIGURE 3. Variation of the total energy of the K–XO$^+$ complex versus the XO Mulliken dipole value in the vibrational excited states of XO, where X = C or N. NO: filled circles, CO: open circles.

knowledge, no data for the latter about such phenomenon, as is well known for the TMCs.

In the future, it is planned to repeat the same analysis with a more precise determination of the dipole value via the distributed multipole analysis scheme of Stone [23] as supplied in the GAMESS code. This scheme requires, however, an additional recalculation to evaluate the multipole moments of any subsystem including the XO ligand. The absence of DFT potentials in GAMESS imposed on us the application of the MP2 electron correlation level only, which is indeed not the best solution. As a consequence of the underestimated slope of the CO dipole in the gas state with MP2, the ΔU dependence with the dipole is also distorted in the carbonyl complexes. The explanation of the vibronic coupling could be sought.

If as mentioned above we succeeded in comparing the CO and NO monocomplexes, the same comparison cannot, however, be realized for the biligand complexes. Binitrosyls indeed lead easily to (NO)$_2$ dimers, in which both N–O vibrations are strongly coupled, and, therefore, the simple estimation of ΔU with Eq. (1) becomes hindered. This dimerization is effective enough so that we never could obtain any stable linear ON–Na$^+$–NO geometry without imaginary frequencies. The global minimum is obtained for an ON–Na$^+$–NO configuration which is very close to the "pure" (NO)$_2$ dimer, i.e., N–N = 1.957 Å, N–O = 1.146 Å, and N–N–O = 101°1 for the cation complex shifted to 2.023 Å, 1.136 Å, and 100°0 in the dimer, the experimental values being 2.263 Å, 1.152 Å, and 97°17, respectively [24, 25].

An opposite behavior was observed for the bicarbonyls; a stable linear OC–Na$^+$–CO geometry was indeed obtained irrespective of the starting configuration (even a small C–Na–C angle of 60° starting with the Na–C distance of 2.8 Å was tested). Na(CO)$_n^+$ complexes, $n > 1$, were often subjects of discussion for the assignment of the C–O vibrational peaks measured within various zeolites [1, 2]. The internal structure of most zeolite framewokes does not allow the formation of linear dimers; so angular dimers could be reasonable candidates. Recently, the (^{15}N$_2$)Na(CO)$^+$ monocarbonyl was proposed in order to explain the band at 2167 cm^{-1} in the area of the C–O vibrational band recorded for CO/^{15}N$_2$ mixtures adsorbed in NaY zeolite [3]. The geometry of the isolated (N$_2$)Na(CO)$^+$ complex is almost linear, i.e., N–Na–C angle of 173°2. The overestimated electric field due to the cation increases the "field-induced" absorption. This leads to a calcu-

lated intensity ratio for the C–O/N–N vibrational bands of only 2.5 while usually this experimental ratio is higher. The intensity of the symmetric band, which is forbidden in linear bicarbonyls, is not that negligible for an angular geometry and should be visible in the recorded spectra.

As soon as the CO–CO interaction is very weak (around 0.44 kcal/mol [26]), the interaction of the CO molecules with any other available adsorption sites of an adsorbent should dominate over the formation of the $Me(CO)_2^+$ complexes. No stable $(CO)_2$ dimers in the case of adsorption on a NaCl surface were theoretically observed with accurate CO–CO potentials [27], while $(NO)_2$ dimers coordinated to the Li cation over a LiCl surface were the object of numerous experimental studies [28]. From the known behavior of the isosteric heat versus the CO coverage in various zeolites, as for A zeolites [29] or CdY [30], one can conclude that the interaction energy between the favored Na site and CO or between the less attractive adsorption sites and CO are both larger than the attractive CO–CO interaction [26]. Despite the attractive dipole–dipole CO–CO interaction for the CO–Na^+–CO complex, with CO differently attached via the O or C terms, no angular form was never obtained. Indirectly, the idea of the presence of bicarbonyls in zeolites means the domination of the electrostatic interaction terms. At the same time, the calculated difference of 2.97 kcal/mol between the total energies of the linear CO–Na^+–CO and OC–Na^+–CO complexes is much larger than the experimental enthalpy difference of 0.9 kcal/mol for the Na^+–CO and Na^+–OC adsorptions measured in NaZSM-5 [31]. This last comparison demonstrates the extent of compensation of the electrostatic field near the Na cation by the framework O atoms. As soon as the field is strongly compensated near the cation, the competitive interaction with the rest of the framework seems to be preferential as compared to the already occupied cation.

The stabilization of the above-mentioned angular geometry owing to the dominant CO–zeolite interaction coud be proposed naturally, but the resulting CO localization would lead to complexes only conventionally named as a bi- or polycarbonyl. Similar types of stabilization for a $Ba(H_2O)_4^{2+}$ pyramidal cluster were observed by us in the hydrated form of the BaEDI zeolite [32]. Even if this pyramidal $Ba(H_2O)_4^{2+}$ geometry corresponds to a local minimum in the gas state, the H_2O molecules experience dominant interactions with the zeolite framework.

As a result, the final H_2O localization agrees only formally with the gas state geometry.

The isobestic point of the proposed bi- and poly-complexation reactions of CO near an alkali cation in zeolites slightly moves with coverage [1, 2]. Hence, we believe that one should argue that the second CO molecule adsorbs in the proximity of the first one as well as of the cation, rather than to assign the second lower vibrational frequency band, i.e., $2164\ cm^{-1}$ in NaETS-10 and $2159\ cm^{-1}$ in NaFER, to a CO molecule coordinated to the same cation. The slight shift of the isobestic point together with a shift of the high-frequency band toward lower frequency at high coverage are in agreement with such proposition. Also, this is in agreement with the conclusion of a lower electrostatic field for the next arriving molecule [2].

Conclusions

The stability of alkali metal complexes $Me(XO)_n^+$, where Me = Li, Na, K, or Rb, and X = C or N, with respect to the vibrational excitation of the XO ligands has been studied at the DFT and MP2 theoretical levels with high-quality basis sets. We have shown that the dipole of the CO and NO ligands behaves similarly in such complexes, but a larger increase of the repulsive electrostatic interaction after the change of the dipole's sign owing to the XO vibrational excitation appears for lower vibrational states in the case of CO versus NO. This result allows to predict CO dissociation from the electronically excited states of the alkali metal complexes $Me(XO)_n^+$ provided that electronic-vibrational coupling exists. For transition metal carbonyls, which present a weak π back-donation, CO can also be eliminated via vibrational excitation from the excited electronic states of the complex.

The possibility of an angular geometry for some bicarbonyls in the gas phase was not supported. The absence of stable angular $Me(CO)_2^+$ complex at the theoretical level does indeed not support the assignment of several vibrational frequency bands to the presence of the complex. We therefore believe that the second CO molecule adsorbed in the same cage of Me-exchanged zeolite forms is not attached to the same Me^+ cation but is positioned in the vicinity of both the cation and the first CO molecule.

References

1. Zecchina, A.; Otero Arean, C.; Turnes Palomino, G.; Geobaldo, F.; Lamberti, C.; Spoto, G.; Bordiga, S. Chem Phys Chem Phys 1999, 1, 1649.

2. Bordiga, S.; Turnes Palomino, G.; Paze, C.; Zecchina, A. Micropor Mesopor Mater 2000, 34, 67.

3. Hadjiivanov, K.; Knözinger, H. Chem Phys Lett 1999, 303, 513.

4. Staemmler, V. Chem Phys 1975, 7, 17.

5. Ikuta, S. Chem Phys Lett 1984, 109, 550.

6. Del Bene, J. E. J Comput Chem 1986, 7, 259.

7. Walter, D.; Sievers, M. R.; Armentrout, P. B. Int J Mass Spectromet Ion Proc 1998, 175, 93.

8. Larin, A. V.; Trubnikov, D. N.; Vercauteren, D. P. Chem Phys Lett, submitted.

9. Löwdin, P. O. J Chem Phys 1950, 8, 365.

10. Mulliken, R. S. J Chem Phys 1955, 23, 1833.

11. Frisch, M. J.; Trucks, G. W.; Schlegel, H. B.; Scuseria, G. E.; Robb, M. A.; Cheeseman, J. R.; Zakrzewski, V. G.; Montgomery, J. A., Jr.; Stratmann, R. E.; Burant, J. C.; Dapprich, S.; Millam, J. M.; Daniels, A. D.; Kudin, K. N.; Strain, M. C.; Farkas, O.; Tomasi, J.; Barone, V.; Cossi, M.; Cammi, R.; Mennucci, B.; Pomelli, C.; Adamo, C.; Clifford, S.; Ochterski, J.; Petersson, G. A.; Ayala, P. Y.; Cui, Q.; Morokuma, K.; Malick, D. K.; Rabuck, A. D.; Raghavachari, K.; Foresman, J. B.; Cioslowski, J.; Ortiz, J. V.; Baboul, A. G.; Stefanov, B. B.; Liu, G.; Liashenko, A.; Piskorz, P.; Komaromi, I.; Gomperts, R.; Martin, R. L.; Fox, D. J.; Keith, T.; Al-Laham, M. A.; Peng, C. Y.; Nanayakkara, A.; Gonzalez, C.; Challacombe, M.; Gill, P. M. W.; Johnson, B.; Chen, W.; Wong, M. W.; Andres, J. L.; Gonzalez, C.; Head-Gordon, M.; Replogle, E. S.; Pople, J. A. Gaussian 98, Revision A.7; Gaussian: Pittsburgh, 1998.

12. Schmidt, M. W.; Baldridge, K. K.; Boatz, J. A.; Elbert, S. T.; Gordon, M. S.; Jensen, J. H.; Koseki, S.; Matsunaga, N.; Nguyen, K. A.; Su, S. J.; Windus, T. L.; Dupuis, M.; Montgomery, J. A. J Comput Chem 1993, 14, 1347.

13. Rauhut, G.; Pulay, P. J Phys Chem 1995, 99, 3093.

14. Maroulis, G. J Phys Chem 1996, 100, 13466.

15. Herzberg, G. Spectra of Diatomic Molecules; Van Nostrand: Princeton, 1950.

16. Muenter, J. S. J Mol Spectrosc 1975, 55, 490.

17. Neumann, R. M. Astrophys J 1970, 161, 779.

18. Hulburt, H. M.; Hirschfelder, J. O. J Chem Phys 1941, 9, 61.

19. Le Roy, R. J. LEVELS program, Dept. of Chem., University of Waterloo, Waterloo, Ontario N2L 3G1, Canada, 1989.

20. Camacho, J. J.; Pardo, A.; Poyato, J. M. L. J Chem Soc Faraday Trans 1994, 90, 23.

21. Castelman, A. W., Jr.; Peterson, K. I.; Upschulte, B. L.; Schelling, F. J. Int J Mass Spectrom Ion Phys 1983, 47, 203.

22. Billingsley, F. P.; Krauss, M. J Chem Phys 1974, 60, 2767.

23. Stone, A. J. Chem Phys Lett 1981, 83, 233.

24. McKellar, A. R. W.; Watson, J. K. G.; Howard, B. J. Mol Phys 1995, 86, 273.

25. Watson, J. K. G.; McKellar, A. R. W. Can J Phys 1997, 75, 181.

26. Rode, M.; Sadlej, J.; Moszynski, R.; Wormer, P. E. S.; van der Avoird, A. Chem Phys Lett 1999, 314, 326.

27. Meredith, A. W.; Stone, A. J. J Chem Phys 1996, 104, 3058.

28. Jackson, R. C.; Polanyi, J. C.; Sjovall, P. J Chem Phys 1995, 102, 6308.

29. Masuda, T.; Tsutsumi, K.; Takahashi, H. J Coll Interf Sci 1980, 77, 238.

30. Boddenberg, B.; Sprang, T. J Chem Soc Faraday Trans II, 1995, 91, 163.

31. Otero Arean, C.; Tsyganenko, A. A.; Escalona Platero, E.; Garrone, E.; Zecchina, A. Angew Chem Int Ed 1998, 37, 3161.

32. Larin, A. V.; Vercauteren, D. P. Stud Surf Sci Cat, 2001, 135, 263.